Determination of scaling exponents in Ag(100) homoepitaxy with x-ray diffraction profiles

J. Alvarez, E. Lundgren, X. Torrelles, and S. Ferrer
European Synchrotron Radiation Facility, Boîte Postale 220, 38043 Grenoble Cedex, France
(Received 26 November 1997)

Homoepitaxy of Ag(100) at different temperatures has been studied by collecting the angular distribution of the intensities of *x* rays diffracted from the growing film, in real time without interruption of the growth at relatively high growth rates (one atomic layer every 80 seconds). The temporal evolution of the long- and medium-range surface correlations has been used to determine the coarsening and roughening exponents at different temperatures. A simple phenomenological model based on rate equations has been found accurately to fit the data. The results suggest that the energy barrier to descend steps is small. [S0163-1829(98)01811-6]

Diffraction techniques based on electrons, neutral atoms, or x rays have been extensively used in the last years to study the epitaxial growth of thin films.[1] Under the appropriate scattering conditions the diffracted intensity may show an oscillatory behavior with a period equal to the time required to the growth of one atomic layer. This has traditionally been interpreted as a consequence of the temporal oscillations of the density of surface atomic steps that occur during the nucleation, growth, and coalescence of two-dimensional islands. In most cases the amplitude of the oscillations of the diffracted intensity exhibits a damping that causes the oscillations to disappear after a certain time. The intensity reaches a nonzero stationary value that reveals a constant step density that is characteristic to the so-called step flow growth in which the deposited atoms do not nucleate new islands but migrate to the neighboring steps.

In most cases the time-resolved diffraction experiments have been done by collecting the most intense and sharp part of the angular distribution of the diffracted intensity that informs on long-range correlations on the surface. More recently, a number of growth experiments[2–7] have measured broader angular profiles of the diffracted intensities, (spot profile analysis) in order to gain insight on the medium-range correlations of the surfaces as may be the distances between the islands. Contrary to the studies of the time dependence of the intensity of the central peak, spot profile measurements have been, in general, performed by interrupting the growth while the diffracted intensity was measured. There is only one exception known by us,[3] but in that case the growth rate was extremely low. Interrupting the growth means, in principle, a profound alteration of the detailed balances between the rates of the different surface processes that may alter some physical aspects of the growth problem unless the temperatures are sufficiently low to prevent significant mass transport on the surface.

Here we report on noninterrupted growth experiments on transverse profile analysis done by diffracting x rays at very grazing angles. For practical reasons, we were interested in growing the films at rates as close as possible to those usually employed in thin-film technology (of the order of one atomic layer every 10 s). With the help of a charge-coupled device (CCD) camera, transverse profiles of the diffracted intensity were recorded with an exposure time to the beam of only two seconds, allowing to monitor in detail the homoepitaxial growth of Ag(100) at rates of 80 s per atomic layer. As a result of these measurements several scaling parameters of the growth were determined. The data allow to directly extract the values of the coarsening exponent that informs on the temporal variation of the medium-range correlations on the surface (the distances between the islands) for a variety of temperatures ranging from 140 to 365 K. Further analysis of the experiments allows to evaluate the numerical values of the roughening exponent at different temperatures. This has been possible by taking advantage of the weak interaction of x rays with the surface that causes the kinematical approximation for the scattering to be valid (in contrast with electron diffraction). Thus, the intensities of the central peak have been evaluated with a simple model consisting in a set of coupled rate equations containing the populations of the different atomic levels that exist on the surface during growth. The resulting diffracted intensities evaluated with our model fit the measurements very accurately (we have not found in the literature similar accurate fits) and allow to determine that the roughening exponent varies from 0.05 to 0.11 in the temperature range of our measurements. In addition, from the fit to the data, it has been found that the interlayer transport between surface levels has an activation energy of 90 meV that might be an indication of a low Schwoebel barrier for adatoms descending atomic steps.

The experiments were performed at the Surface Diffraction beamline (ID3) at the European Synchroton Radiation Facility that has been described previously.[8] The end station consist of an ultrahigh-vacuum chamber coupled to a high precision diffractometer. Prior to installation into the vacuum chamber, the Ag(100) crystal was etched with a mixture of nitric and hydrofluorhidric acids. In the vacuum, it was prepared by successive cycles of ion etching and annealing until terraces of ~ 2000 Å lateral dimensions were obtained as indicated by the width of the diffracted beams. The temperature of the crystal was measured with a thermocouple in contact with the crystal. Ag was evaporated from a commercial Knudsen cell. The crystal lattice was described with a basis a_1, a_2, a_3 with a_1, a_2 in the (100) plane and a_3 along [100]. Their magnitudes are $a_1 = a_2 =$ nearest-neighbor distance $= a_0/\sqrt{2}$ and $a_3 = a_0$ ($a_0 =$ bulk lattice constant). With this basis, Bragg conditions are fulfilled at $(H,K) = (1,0)$ and $L = 1,3,5 \ldots$. By setting the scattering vector at (1,0,0), the phase difference between two consecutive (100)

 © 1998 The American Physical Society

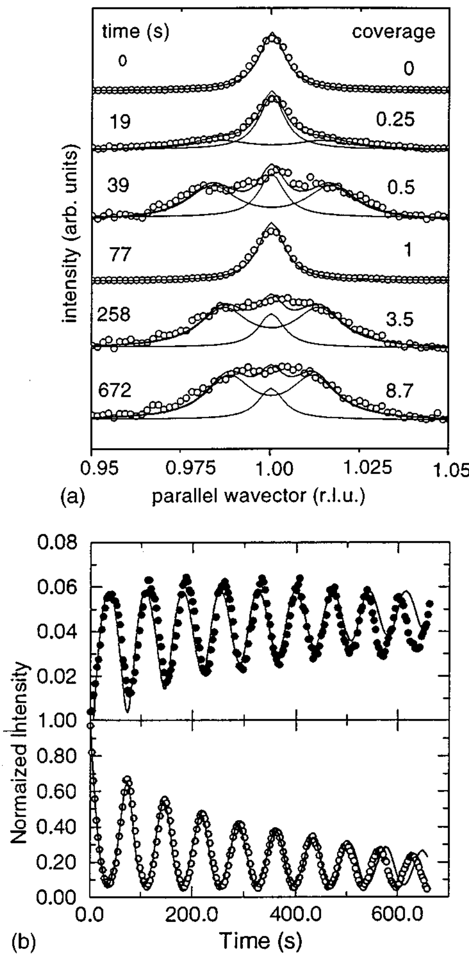

FIG. 1. (a) Temporal evolution of the angular distribution of the diffracted intensity during growth of Ag(100) at 313 K. The deposition time and the corresponding coverages (in atomic layers) are indicated. The different curves are not drawn to the same scale. Each profile was recorded in 3.5 s (2 s exposure time plus 1.5 s redout time). The continuous lines are Lorentzian fits to the data. (b) Temporal evolution of the intensities of the central peak (bottom) and diffuse peaks (top). Note the different ordinate scales. The continuous lines are fits using the model described in Eqs. (1) and (2) in the text.

planes of the crystal is π and the corresponding amplitudes cancel each other. As it has been discussed in the literature, these are suitable conditions for epitaxial growth experiments since the sensitivity to surface atomic steps is highest. Our measurements were performed at $L<0.1$, which corresponds to grazing incidence and exit angles (about 0.1 degrees). The diffracted line profiles were collected with a binned CCD camera mounted in the detector arm of the diffractometer. It was equipped with a phosphorous screen and a tapered fiber optics as focusing stage allowing to collect x rays within a solid angle of ~ 6 mstereorad from the sample.

Figure 1(a) shows several representative profiles during the growth at 310 K. The diffuse scattering at symmetric positions from the central peak is most clear at fractional coverages due to the higher density of steps. The profiles have been decomposed into three Lorentzian components as shown in the figure. the Lorentzian describing the central peak at $H=1.00$ has been obtained by fitting the data at $t=0$ and letting only a scale factor as free parameter for the

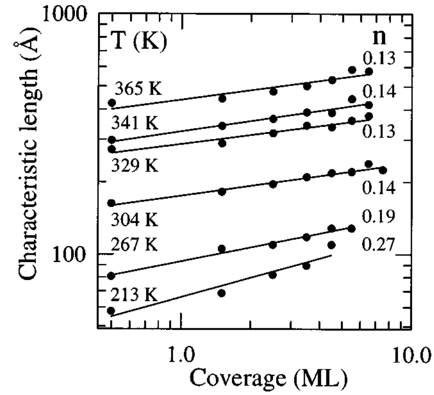

FIG. 2. Characteristic lengths derived from the positions in reciprocal space of the diffuse intensities, as a function of fractional coverages for growth at different temperatures. The slopes of the adjusted lines give the values of the coarsening exponents n.

profiles at $t\neq 0$. The diffuse peaks have been adjusted with two components, symmetric with respect to the central peak, having positions, widths and intensities as free parameters to fit the data. Figure 1(b) displays the temporal evolution of the intensities of the central and diffuse peaks as obtained from fits to the raw data. The central peak exhibits the familiar damped oscillations with periodicity of one atomic layer. The diffuse intensity, much weaker, shows also an oscillatory behaviour with a phase lag of half oscillation with respect to the central peak. The intensity of the diffuse peak is maxima at coverages $\frac{1}{2}$, $\frac{3}{2}$, $\frac{5}{2}$ ... where the density of steps is higher and the intensity of the central peak shows minima. The separation ΔH of the diffuse components and the central peak directly informs on the distances between islands on the surface.

Figure 2 summarizes our results at different growth temperatures. The characteristic length in the ordinates defined as $2\pi/\Delta H$, has been plotted as a function of the deposited coverage. The data points on the figure correspond to fractional coverages $\frac{1}{2}$, $\frac{3}{2}$, $\frac{5}{2}\cdots$ since for these values, as the intensity of the diffuse component relative to the central one is large, the deconvolution described above is better. At a coverage of 0.5 layers, the characteristic length varies from 60 to 400 Å in the temperature range investigated. Evaluation of the effective energy determining that variation may be achieved by evaluating the slope of log(characteristic length) vs $1/T$. This results in 62 ± 2 meV that is similar to previously published values in epitaxial growth of Cu(100) that were found to be around 70 meV.[6] The same exercise at a deposited coverage of 5.5 layers results in the slightly smaller energy of 58 ± 3 meV.

For a fixed temperature, the increase of the characteristic length with coverage displayed in the figure, is usually described with the help of the scaling exponents describing growth processes. The one relevant here is the coarsening exponent n defined from (charac. length)$\propto t^n$. The slopes of the lines that fit the data in the figure give the values of n for different temperatures. They range from 0.27 to 0.13 that may be compared to $n=0.23$ found in Ref. 7 for Cu(100) growth at room temperature. Previously published work by Amar and Family[9] on Montecarlo simulations of the growth process on a metallic substrate, indicate that the numerical

values of the coarsening exponent depend markedly on the magnitude of the step barrier to interlayer diffusion. According to those simulations, at temperatures around 300 K, large (~ 0.6 eV) Schwoebel barriers result in n values of ~ 0.33 whereas low barriers (~ 0.07 eV) give $n \sim 0.16$. On this basis, our findings would suggest a low step barrier height although this may be controversial since it does not quite agree with the results in Ref. 7. To extract additional information from the experimental data, we now turn to a more sophisticated data analysis.

The continuous line that fits the temporal evolution of the intensity of the central component displayed in Fig. 1(b) lower panel, has been evaluated with a modified version of a model due to Cohen *et al.*[10] and with the use of the kinematical approximation in the scattered intensity. Our model does not deal with the different microscopic steps in the growth process (as for example in Ref. 11) but only pretends to produce a phenomenological description of the distribution of levels in the growing film.

Suppose an initially flat and perfect substrate on top of which a film is epitaxially growing. For an ideally perfect layer-by-layer growth, only two levels would exist on the surface. In reality, due to the limited mass transport, several levels will simultaneously coexist and grow. The concentration of a certain level i, θ_i, will vary with time as a result of three processes: the direct impingement of atoms coming from the vapor, the atoms that descend from the level $i+1$ and the atoms that leave the level i and descend to the level i-1. This may be expressed by a set of rate equations:

$$d\theta_i/dt = (1/\tau)(\theta_{i-1} - \theta_i) + k(t)\theta_{i+1}(\theta_{i-1} - \theta_i) - k(t)\theta_i(\theta_{i-2} - \theta_{i-1}), \quad (1)$$

where $1/\tau$ and $k(t)$ are the rates of deposition and of interlayer transport, respectively. multiplied by the corresponding concentration factors. For example, the transport of an atom from level $i+1$ to leave i requires atoms in level $i+1$ (θ_{i+1}) and empty space in level i ($\theta_{i-1} - \theta_i$).

As mentioned above, scaling laws applied to the growth process, described, in general, relevant parameters of the surface morphology (as for example the roughness) in the form of temporal power laws. Based on that, the rate of interlayer transport $k(t)$ has been assumed to obey a power law of the form

$$k(t) = A/t^m, \quad (2)$$

where A and m are adjustable parameters. Other functional forms of $k(t)$ were tried with less success in reproducing the experiments. Although its microscopical understanding is still in progress, Eq. (2) naturally will cause that after long growing times the interlayer transport will vanish and the film will grow by attachment of the atoms from the vapor to pre-existing steps causing step displacements and a stationary step concentration. Also, the pre-exponential term A should be expected to increase with temperature due to the enhancement of mass transport at elevated growth temperatures.

If the temporal dependence of the coverages of different levels θ_i is known, one may evaluate the diffracted intensity of the central component as

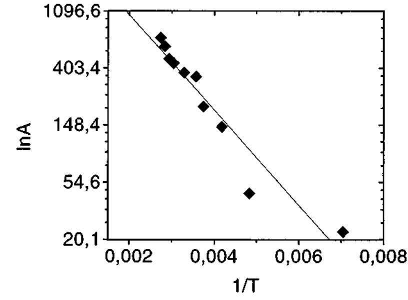

FIG. 3. Arrhenius plot of the preexponential factor of Eq. (2). The slope results in an energy of 90 meV.

$$I_{\text{central peak}}(t) \propto [\tfrac{1}{2} - \delta(t)]^2, \quad (3)$$

where $\delta(t)$ is defined as $\delta(t) = \theta_1 - \theta_2 + \theta_3 - \theta_4 \ldots$. The alternance of signs in the consecutive coverages origins from the π phase shift between consecutive layers and the term $\frac{1}{2}$ from the contribution of the substrate.[12]

The data in Fig. 1(b) have been fitted minimising the residuals (mean absolute relative errors) between the experiment and the calculation while A and m were varied. For every pair of (A,m) values, the set of Eqs. (1) was solved, $I_{\text{central peak}}(t)$ was evaluated with Eq. (3) and the agreement with the experiment was calculated.

The values of A are affected by an undetermined scale factor which causes that only its relative changes with temperature have to be considered. The calculated curve in Fig. 1(b) has $m = 0.99$. The residual is 0.17.

This procedure was applied to a set of ten different growth experiments with temperatures between 140 and 365 K. The residual of the fits were comparable to that in Fig. 1(b) and ranged from 0.11 and 0.27. The average value of m and its standard deviation were found to be $m = 1.00 \pm 0.06$. The best fit values of A at different temperatures are displayed in Fig. 3. As it may be seen the pre-exponential fol-

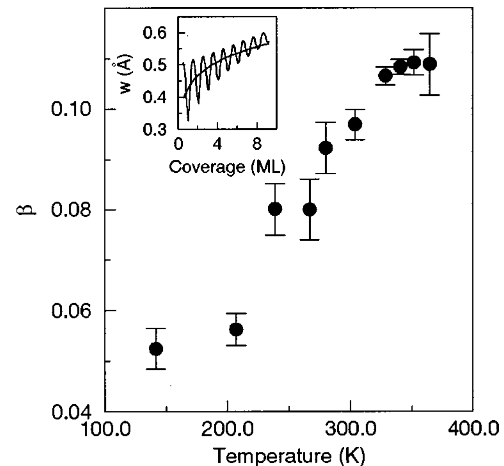

FIG. 4. Inset: Evolution of the roughness w, in angstroms, with film thickness for growth at 313 K. The monotonously increasing curve is a fit with $\langle w \rangle \propto t^\beta$, as explained in the text, and it allows to extract the roughening exponent β. Main figure: Dependence β with growth temperature.

lows an Arrhenius type of activated behavior. The slope of the data gives an energy of 90 ± 9 meV.

The temporal evolution of the diffuse intensity displayed in the top panel of Fig. 1(b), may be shown to be described by $I_{\mathrm{diffuse}}\propto \delta(t)[1-\delta(t)]$.[13] The continuous curve in the figure shows the results obtained by using the $\delta(t)$ values obtained from the fit of the central component. The agreement with the experiment is worse than that of the central component probably due to the fact that as the diffuse intensity is in general much weaker than the central one, the accuracy of the fits is worst.

The distribution of surface levels resulting from the solutions of Eq. (1) may be used to evaluate the surface rms roughness $w=(\langle h^2\rangle-\langle h\rangle^2)^{1/2}$ with $\langle h\rangle=\Sigma j(\theta_j-\theta_{j+1})$ and $\langle h^2\rangle=\Sigma j^2(\theta_j-\theta_{j+1})$. The inset of Fig. 4 shows w as a function of coverage for the growth at 313 K. The oscillatory behavior of w reflects the oscillatory step concentration. The temporal evolution of the average roughness may be evaluated by simply averaging the values of w at the local maxima and minima as in Ref. 9. The resulting average roughness $\langle w\rangle$ is described by the scaling law $\langle w\rangle\propto t^{\beta}$ where β is the roughening exponent which may be deduced from the slope of the straight line in the inset of Fig. 4. The values of β for different growth temperatures are displayed in Fig. 4. As it may be observed they increases with increasing temperatures from 0.05 to 0.11. These values should be compared with the simulations in Ref. 9 that result in values of β about 0.08 for growth processes involving small or negligible step barriers and values of β about 0.31 for large step barriers. Again, our data are consistent with a small step barrier.

Although the microscopic origin of Eq. (2) has not been established yet, the activation energy (90 meV) deduced from the temperature dependence of A, could be tentatively taken as an upper limit of the magnitude of the Schwoebel barrier. Recent density-functional theory studies[14] predict no additional energy barrier to descend a step in qualitative agreement with our findings.

In summary, noninterrupted growth experiments of Ag(100) have been performed by measuring the transverse distribution of diffracted intensity. A phenomenological model involving rate equations and a power law dependence of the interlayer transport rate, has been found to accurately describe the temporal evolution of the diffracted intensity. The values of the coarsening and roughening exponents at different temperatures have been determined and suggest a small energy barrier at the steps.

[1] For a review, see for example, B. A. Joyce, J. M. Neave, J. Zhong, P. J. Dobson, P. Dawson, K. J. Moore, and C. T. Foxon, in *Thin Film Growth Techniques for Low Dimensional Structures* Vol. 163 of *NATO Advanced Study Institute*, Series B: Physics, edited by R. F. C. Farrow, S. S. Parkin, P. J. Dobson, J. H. Neave, and A. S. Arrot (Plenum, New York, 1987).

[2] M. Henzler, H. Busch, and G. Friese, in *Kinetics of Ordering and Growth at Surfaces*, edited by M. G. Lagally (Plenum, New York, 1990), and also G. L. Nyberg, M. T. Kief, and W. F. Egelhoff, Jr., Phys. Rev. B **48**, 14 509 (1993).

[3] J. K. Zuo, J. F. Wendelken, H. Durr, and C. L. Liu, Phys. Rev. Lett. **72**, 3064 (1994).

[4] H. J. Ernst, F. Fabre, and J. Lapoujulade, J. Vac. Sci. Technol. A **12**, 1809 (1994).

[5] B. Grossman and P. Piercy, Phys. Rev. Lett. **74**, 4487 (1995).

[6] L. C. Jorritsma, M. Bijnagte, G. Rosenfeld, and B. Poelsema, Phys. Rev. Lett. **78**, 911 (1997).

[7] J. K. Zuo and J. F. Wendelken, Phys. Rev. Lett. **78**, 2791 (1997).

[8] S. Ferrer and F. Comin, Rev. Sci. Instrum. **66**, 1674 (1995).

[9] J. G. Amar and F. Family, Phys. Rev. B **54**, 14 742 (1996).

[10] P. I. Cohen, G. S. Petrich, P. R. Pukite, G. J. Whaley, and A. S. Arrot, Surf. Sci. **216**, 222 (1980).

[11] M. C. Bartelt and J. W. Evans, Phys. Rev. Lett. **75**, 4250 (1995), and J. W. Evans and M. C. Bartelt, Langmuir **12**, 217 (1996).

[12] I. K. Robinson, *Handbook of Synchrotron Radiation, Vol. 3* (North-Holland, Amsterdam, 1991).

[13] J. M. Cowley, *Diffraction Physics* (North-Holland, Amsterdam, 1990), Chap. 7.

[14] B. D. Yu and M. Scheffler, Phys. Rev. Lett. **77**, 1095 (1996).